Synthesis of axially di- and peripherally tetra-(4-{[(1E)-(4-methoxyphenyl) methylene]amino}phenoxy) group substituted metallophthalocyanines and their electrochemistry

Hüseyin Baş* iD , Zekeriya Bıyıklıoğlu iD

Karadeniz Technical University, Faculty of Science, Department of Chemistry, 61080, Trabzon, Türkiye

Abstract

In this study, the new phthalonitrile derivative, axially di-(4-{[(1E)-(4-methoxyphenyl)methylene]amino}phenoxy) substituted Si(IV) phthalocyanine and peripherally tetra-(4-{[(1E)-(4-methoxyphenyl)methylene]amino}phenoxy) substituted Cu(II), Mn(III) phthalocyanines have been synthesized and characterized. Then electrochemical measurements of axially di- and peripherally tetra-(4-{[(1E)-(4-methoxyphenyl)methylene]amino}phenoxy) group substituted Si(IV), Cu(II), Mn(III) phthalocyanines were investigated with cyclic voltammogram (CV) technique. The redox properties of Si(IV), Cu(II), Mn(III) phthalocyanines show that Mn^{III} center into the Pc cavity increased the redox richness of the phthalocyanines, with the addition of metal-based electron transfer processes to the ring-based ones while Si^{IV} and Cu^{II} show only ring-based electron transfer processes.

Keywords: Synthesis, phthalocyanine, silicon, manganese, cyclic voltammetry

1. Introduction

Phthalocyanines, which obey the Huckel rule (4n+2) with their 18-π electron system, constitute a unique class of macro heterocyclic compounds [1]. They are high-conjugated synthetic macrocyclic compounds containing four isoindole units with 18 π electrons [2]. Also have very good thermal and chemical stability [3]. Because of their distinctive chemical structures and full aromatic delocalization, they are widely popular and used in many high-tech industries. [4]. For example, it is used in many fields such as thin film [5], non-linear optics (NLO) [6,7], dye-sensitized solar cells (DSSCs) [8,9], electrochemistry [10–12], photodynamic therapy (PDT) [13–15]. Although these compounds have a wide range of applications, they have low solubility and a high tendency to aggregate [16]. In other words, Pcs are poorly soluble in common organic solvents [17]. The synthesis of soluble Pcs by adding functional groups to the molecule has therefore been the focus of much research. Pcs can be easily substituted from peripheral, non-peripheral and axial positions [18]. The kind of the central metal atom and the location of the substituents on the phthalocyanine ring are used to categorize

phthalocyanines [19]. Tetra-substituted Pcs can be produced by various substitutions of peripheral or non-peripheral regions of the ring structure, while axially substituted ones can be obtained by bonding to the phthalocyanine ring at axial positions on the central metal atom. [20–22].

Phthalocyanines are known to have redox properties [23]. To improve these compounds' suitability for use in various electrochemical applications, it is important to improve the redox activity of metallophthalocyanines (MPcs) [24,25]. Complexation with redox-active metal cations has been observed to boost the redox activity of Pc [26]. The addition of redox-active groups to the Pc ring is another method of improving the redox properties of these molecules. [27,28]. In this way, the absorption of phthalocyanines shifts from the visible region to the near IR or UV region, causing optical transitions. [29,30]. As a result, phthalocyanines electrical and optical characteristics may be controlled and are used in a variety of application, including sensors, dye-sensitized solar cells (DSSCs), nanobiotechnology and nonlinear optics (NLO) [7].
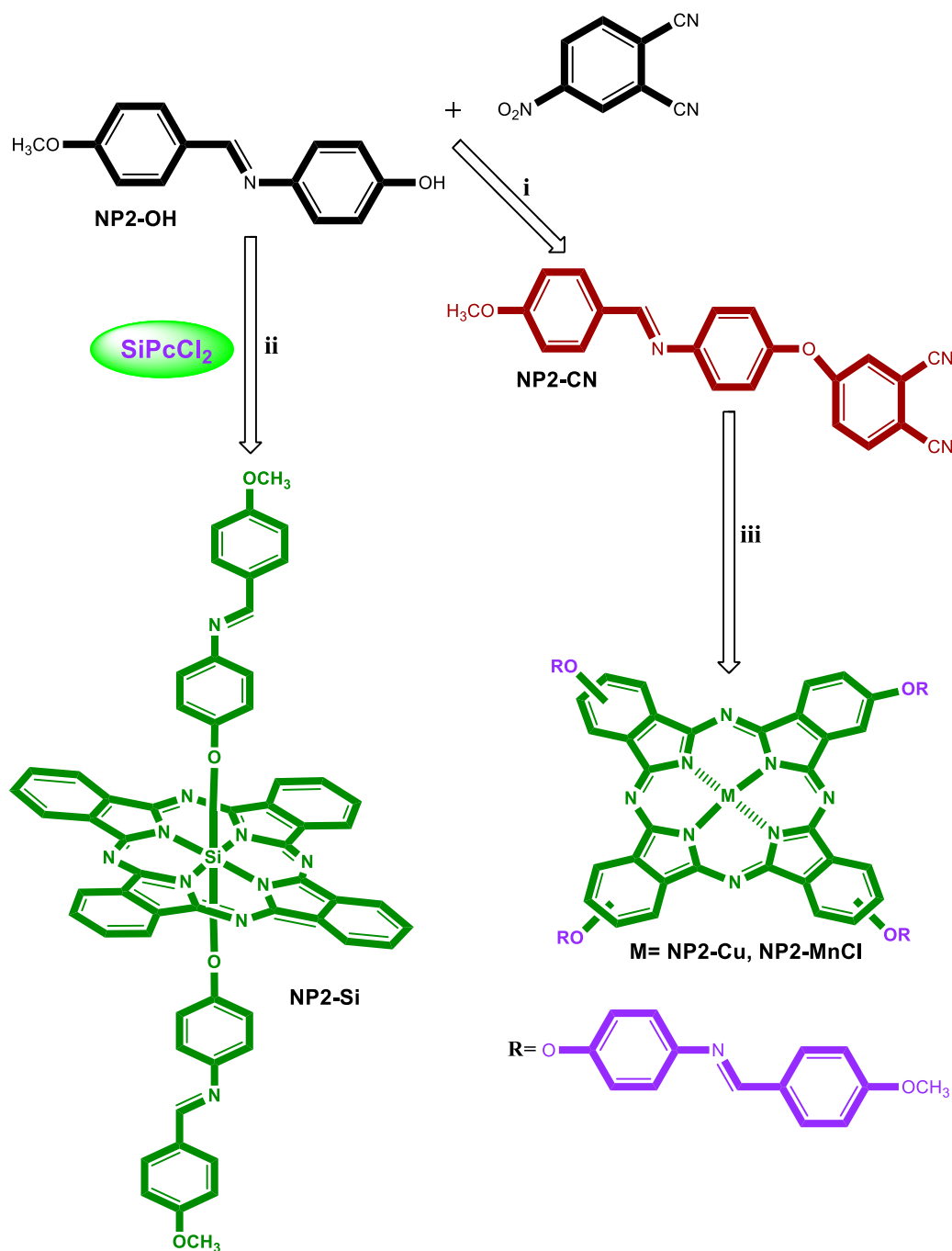
Figure 1. The synthesis of axially di- and peripherally tetra-(4-{[(1*E*)-(4-ethoxyphenyl)methylene]amino}phenoxy) group substituted metallophthalocyanines (i) K₂CO₃, 60 °C, DMF. (ii) Toluene, NaH, 110 °C. (iii) n-pentanol, CuCl₂, MnCl₂, DBU, 160 °C

With this in mind, we have synthesised a new series of phthalocyanine derivatives to investigate their electrochemical properties. The electrochemical properties of the synthesised **NP2-SiPc, NP2-MnPc** and **NP2-CuPc** compounds were determined by cyclic voltammetry (CV) technique.

2. 2. Experimental

2.1. Synthesis

2.1.1. 4-(4-{[(1E)-(4-methoxyphenyl)methylene]amino}phenoxy)phthalonitrile (NP2-CN)

NP2-OH (1.2 g, 5.3 mmol), 4-nitrophthalonitrile (915 mg, 5.3 mmol) and dry K₂CO₃ (2.2 g, 15.9 mmol) were dissolved in anhydrous DMF (20 mL) at 60 °C and under nitrogen atmosphere for stirred 4 days. Then, reaction mixture was poured into water. **NP2-CN** was crystallized from ethanol. Yield: 1.56 g (84%). FT-IR (ATR) v (cm⁻¹): 3077 (Ar-H), 2970-2854 (Aliph. C-H), 2232 (C≡N), 1627, 1601, 1575, 1509, 1481, 1459, 1305, 1279, 1244, 1208, 1176, 1088, 1018, 952, 845, 828, 758. ¹H-NMR (400 MHz, DMSO-d₆), (δ): 8.58 (s, 1H, =CH), 8.12 (d, 1H, Ar-H), 7.91 (d, 2H, Ar-H), 7.80 (s, 1H, Ar-H), 7.42-7.36 (m, 3H, Ar-H), 7.24 7.09 (d, 2H, Ar-H), 7.09 (d, 2H, Ar-H), 3.84 (s, 3H, -OCH₃). ¹³C-NMR (100 MHz, DMSO-d₆),

(δ): 162.48, 161.81, 160.72, 151.87, 149.79, 136.77, 131.00, 129.30, 123.47, 122.93, 122.24, 121.68, 117.15, 116.39, 115.88, 114.76, 108.49, 55.90. MS (ESI), (m/z): 353.44 [M]+.

2.1.2. Synthesis of axially di-(4-{[(1E)-(4-methoxyphenyl) methylene]amino}phenoxy) substituted silicon(IV) phthalocyanine (NP2-Si)

SiPcCl2 (100 mg, 0.16 mmol), **NP2-OH** (75 mg, 0.32 mmol) and NaH (7 mg, 0.32 mmol) in toluene (15 mL) was under nitrogen atmosphere stirred for 1 day at 110 °C. After evaporating the solvent, the product was subjected to column chromatography which is placed aluminium oxide using CHCl3:CH3OH (100:1) as solvent system. Yield: 91 mg (56%). IR (ATR) νmax/cm-1: 3052 (Ar-H), 2961-2850 (Aliph. C-H), 1603, 1575, 1508, 1493, 1429, 1335, 1292, 1254, 1160, 1122, 1095, 1078, 1018, 911, 882, 828, 759, 732. 1H-NMR. (400 MHz, CDCl3), (δ:ppm): 9.65-9.62 (m, 8H, Pc-H$_\alpha$), 8.37-8.35 (m, 8H, Pc-H$_\beta$), 7.85 (d, 4H, Ar-H), 7.49 (s, 2H, Ar-H), 7.01 (d, 4H, Ar-H), 6.75 (d, 4H, Ar-H), 5.53 (d, 4H, Ar-H), 3.75 (s, 3H, -OCH3). 13C-NMR (100 MHz, CDCl3), (δ:ppm): 164.58, 156.82, 149.60, 135.56, 132.00, 131.12, 130.90, 129.78, 123.85, 119.75, 117.79, 114.29, 113.87, 55.58. UV-Vis (THF): λmax, nm (log ε): 676 (5.03), 609 (4.35), 352 (4.74). MALDI-TOF-MS m/z: 993.45 [M]+.

2.1.3. Synthesis of peripherally tetra-(4-{[(1E)-(4-methoxyphenyl)methylene]amino}phenoxy) substituted copper(II) phthalocyanine (NP2-Cu)

NP2-CN (100 mg, 0.28 mmol), dry CuCl2 (19 mg, 0.14 mmol), dry n-pentanol (2 mL) and 1,8-diazabycyclo [5.4.0]undec-7-ene (DBU) (3 drops) was under nitrogen atmosphere stirred at 160 °C for 1 day. Then, **NP2-Cu** was precipitated with ethanol. **NP2-Cu** was purified by column chromatography (aluminum oxide) using CHCl3:CH3OH (100:2) solvent system. Yield: 33 mg (32%). FT-IR (ATR) νmax/cm-1: 3070 (Ar-H), 2919-2849 (Aliph. C-H), 1602, 1574, 1508, 1495, 1464, 1400, 1342, 1311, 1226, 1190, 1161, 1090, 1027, 949, 827, 746. UV-Vis (THF): λmax, nm (log ε) 678 (4.98), 610 (4.46), 337 (5.03). MALDI-TOF-MS m/z: 1476.35 [M]+.

2.1.4. Synthesis of peripherally tetra-(4-{[(1E)-(4-methoxyphenyl)methylene]amino}phenoxy) substituted manganese(III) phthalocyanine chloride (NP2-Mn)

NP2-Mn was prepared using same procedure for the **NP2-Cu** by using dry MnCl2 instead of CuCl2. Yield: 52 mg (50%). FT-IR (ATR) νmax/cm-1: 3034 (Ar-H), 2957-2836 (Aliph. C-H), 1602, 1574, 1508, 1495, 1464, 1399, 1335, 1311, 1225, 1160, 1073, 1026, 951, 886, 826, 743. UV-Vis (THF): λmax, nm (log ε) 723 (4.99), 638 (4.66), 498 (4.32), 342 (5.17). MALDI-TOF-MS m/z: 1468.48 [M-Cl]+.

3. Results and discussion

3.1. Synthesis and characterization

The general synthesis of peripherally tetra- and axially di-(4-{[(1E)-(4-methoxyphenyl) methylene] amino} phenoxy) group substituted metallophthalocyanines is given in Fig. 1. The preparation of **NP2-CN** was succeed by the reaction of 4-{[(1E)-(4-methoxyphenyl) methylene]amino}phenol [31] with 4-nitrophthalonitrile in anhydrous DMF with dry potassium carbonate. Silicon phthalocyanine dichloride was treated with **NP2-OH** in toluene and NaH led to axially di-(4-{[(1E)-(4-methoxyphenyl) methylene] amino} phenoxy) group substituted silicon phthalocyanine. Through a cyclotetramerization reaction in n-pentanol between **NP2-CN** and a metal salt, Cu(II) and Mn(III)Pcs with substituted 4-[(1E)-(4-methoxyphenyl)methylene]ami-nophenoxy) groups were created peripherally. The typical nitrile stretching vibration was visible at 2232 cm-1 when the FT-IR spectra of **NP2-CN** was investigated. The -OH stretching vibration of **NP2-OH** was vanished. Aromatic protons of **NP2-CN** were seen in the 1H-NMR spectrum between 8.12 and 7.09 ppm. Also, =CH and –OCH3 protons were observed at 8.58 and 3.84 ppm, respectively. In the 1H-NMR spectrum of N**P2-CN**, the nitrile carbon atoms of the N**P2-CN**, were observed at 115.88 and 114.76 ppm. In addition, the carbon atom of methoxy group was seen at 55.90 ppm. The molecular ion peak in the mass spectra of **NP2-CN** was seen at m/z: 353.44 [M]+. The removal of the OH band in the IR spectrum provided unmistakable proof that **NP2-Si** had formed. In the 1H NMR spectrum of **NP2-Si,** H$_\alpha$ and H$_\beta$ protons of phthalocyanine ring was shown at 9.65-9.62, 8.37-8.35 ppm, respectively. The other aromatic protons were observed at 7.85, 7.49, 7.01, 6.75, 5.53 ppm. Also, protons of methoxy groups appeared at 3.75 ppm as singlet. In the 13C-NMR spectrum of **NP2-Si** indicated 13 number aromatic and 1 number aliphatic carbon signals. In MALDI-TOF MS spectrum of **NP2-Si**, the molecular ion peak was shown at 993.45 [M]+. The disappearance of the –C≡N vibration (2232 cm-1) in the IR spectrum of **NP2-Cu** and **NP2-Mn** indicated the conversion of **NP2-CN** to the phthalocyanine ring. Owing to the paramagnetic nature of Cu(II) and Mn(III) ion, 1H-NMR and 13C-NMR measurements of **NP2-Cu** and **NP2-Mn** could not be measured [32]. In MALDI-TOF MS spectra of **NP2-Cu** and **NP2-Mn** the molecular ion peaks were found at m/z 1476.35 [M]+, 1468.48 [M-Cl]+, respectively. The UV-Visible spectra of **NP2-Si, NP2-Cu, NP2-Mn** were recorded in THF at 1x10-5 M concentration (Fig. 2). All phthalocyanines (**NP2-Si, NP2-Cu, NP2-Mn**) showed the Q and B bands in the expected ranges. As seen in Fig. 2, the sharp Q bands of **NP2-Si, NP2-Cu, NP2-Mn** were seen at 676, 678, 723 nm, respectively. In addition, the peak at 498 nm for **NP2-Mn** was associated with charge transfer absorption [33]. On the other hand, the B bands of **NP2-Si, NP2-Cu, NP2-Mn** were observed at 352, 337, 342 nm, respectively.
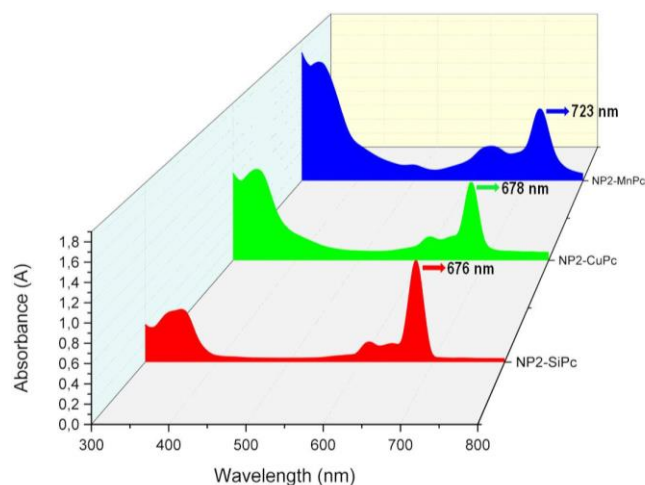
Figure 2. UV-Vis spectrum of **NP2-Si, NP2-Cu, NP2-Mn** in THF. (Concentration = 10×10^{-6} mol dm^{-3})

Figure 5. CV of **NP2-Mn**

Table 1. Electrochemical data of **NP2-Si, NP2-Cu, NP2-Mn**. All potentials were given versus SCE

Pcs	Redox Processes	Label	$^a E_{1/2}$ (V)	$^b \Delta E_P$ (mV)	$^c \Delta E_{1/2}$
NP2-Si	$[L_2Si^{IV}Pc^{2-}]/[L_2Si^{IV}Pc^{3-}]^{1-}$	R$_1$	-0.60	135	
	$[L_2Si^{IV}Pc^{3-}]^{1-}/[L_2Si^{IV}Pc^{4-}]^{2-}$	R$_2$	-1.04	141	1.86
	$[L_2Si^{IV}Pc^{2-}]/[L_2Si^{IV}Pc^{1-}]^{1+}$	O$_1$	1.26	152	
NP2-Cu	$[Cu^{II}Pc^{2-}]/[Cu^{II}Pc^{3-}]^{1-}$	R$_1$	-0.97	202	
	$[Cu^{II}Pc^{3-}]^{1-}/[Cu^{II}Pc^{4-}]^{2-}$	R$_2$	-1.56	154	2.09
	$[Cu^{II}Pc^{2-}]/[Cu^{II}Pc^{1-}]^{1+}$	O$_1$	1.12	156	
NP2-Mn	$[Cl^{1-}Mn^{III}Pc^{2-}]/[Cl^{1-}Mn^{II}Pc^{2-}]^{1-}$	R$_1$	-0.17	96	
	$[Cl^{1-}Mn^{II}Pc^{2-}]^{1-}/[Cl^{1-}Mn^{I}Pc^{2-}]^{2-}$	R$_2$	-1.01	129	
	$[Cl^{1-}Mn^{I}Pc^{2-}]^{2-}/[Cl^{1-}Mn^{I}Pc^{3-}]^{3-}$	R$_3$	-1.51	138	1.29
	$[Cl^{1-}Mn^{III}Pc^{2-}]/[Cl^{1-}Mn^{III}Pc^{1-}]^{1+}$	O$_1$	1.19	141	

^{a}: $E_{1/2}$ values (($E_{pa}+E_{pc}$)/2) were given versus SCE at 0.100 Vs^{-1} scan rate.
^{b}: $\Delta E_P = E_{pa}-E_{pc}$. ^{c}: $\Delta E_{1/2} = E_{1/2}$ (first oxidation)- $E_{1/2}$ (first reduction)
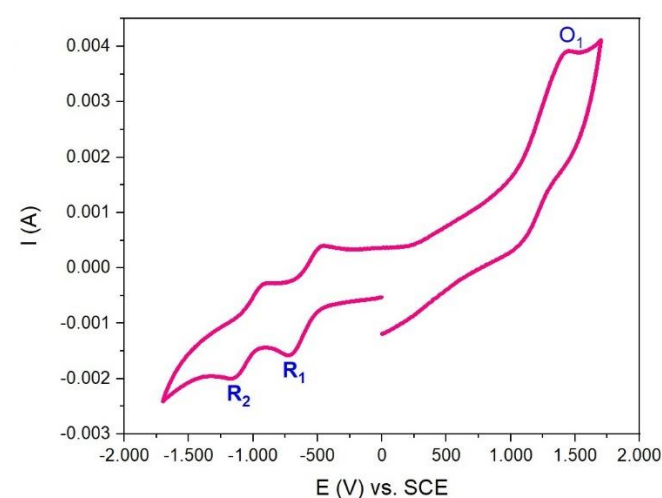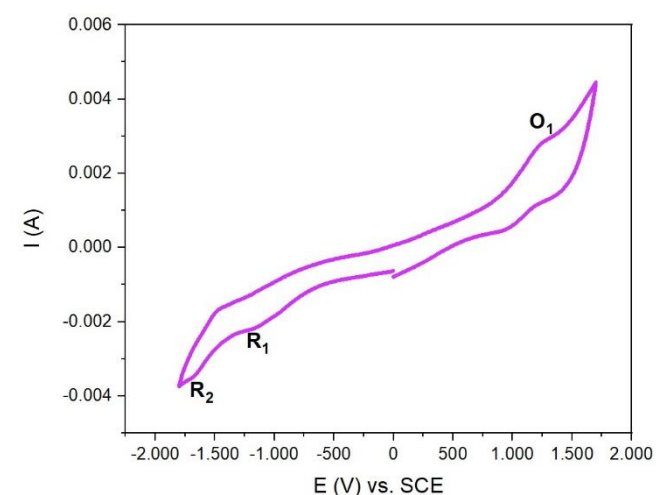

Figure 3. CV of **NP2-Si**

Figure 4. CV of **NP2-Cu**

3.2. Electrochemical Measurements

Electrochemical behaviors of axially di- and peripherally tetra-(4-{[(1*E*)-(4-ethoxyphenyl) methylene] amino} phenoxy) group substituted metallophthalocyanines were recorded using cyclic voltammetry(CV) in DCM/TBAP electrolyte at room temperature. The peak potential separation (ΔE_P), half-wave potential ($E_{1/2}$), the potential difference between the first half-peak processes ($\Delta E_{1/2}$), are shown in Table 1.
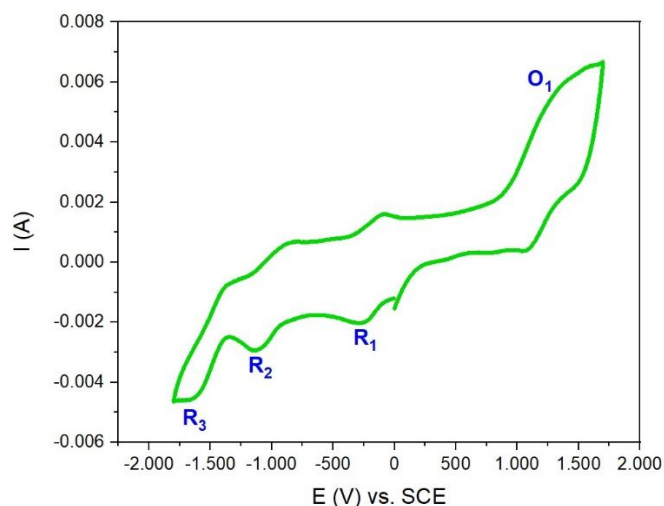
Fig. 3 shows cyclic voltammogram of axially di-(4-{[(1E)-(4-methoxyphenyl)methylene]amino}phenoxy) substituted silicon(IV) phthalocyanine (**NP2-Si**) in DCM/TBAP electrolyte on a Pt working electrode. As shown in Fig. 3, **NP2-Si** illustrated two reduction (R$_1$= -0.60 V, R$_2$= -1.04 V) and one oxidation (O$_1$ = 1.26 V) reaction within the potential windows of the electrolyte. Here, axially di-(4-{[(1E)-(4-methoxyphenyl) methylene] amino}phenoxy) substituted silicon(IV) phthalocyanine (**NP2-Si**) have redox inctive Si^{4+} metal centers. For this reason, **NP2-Si** illustrates only phthalocyanine ring based redox responses and the axial (4-{[(1E)-(4-methoxyphenyl)methylene]amino}ligand on Si center do not considerably influence the redox response of the phthalocyanine ring [34]. According to the peak analyses and shape of the voltammogram, reduction and oxidation processes have quasi-reversible character.

Fig. 4 shows cyclic voltammogram of peripherally tetra-(4-{[(1E)-(4-methoxyphenyl)methylene]amino} phenoxy) substituted copper(II) phthalocyanine (**NP2-Cu**) in DCM/TBAP electrolyte on a Pt working electrode. As shown in Fig. 4, two reduction and one oxidation processes are observed at −0.97 V (R$_1$), −1.04 V (R$_2$), and

1.26 V (O₁) with the cyclic voltammogram of **NP2-Cu**. These redox processes are easily attributed to the electron transfer reaction of phthalocyanine ring owing to the redox inactivity of the Cu²⁺ cation. According to the peak-to-peak separation (ΔE_P), R₁ has irreversible, R₂ and O₁ have quasi-reversible character.

Fig. 5 shows cyclic voltammogram of peripherally tetra-(4-{[(1E)-(4-methoxyphenyl) methylene]amino} phenoxy) substituted manganese(III) phthalocyanine chloride (**NP2 Mn**). Peripherally tetra-(4-{[(1E)-(4-methoxyphenyl)methylene]amino}phenoxy) substituted manganese(III) phthalocyanine chloride (**NP2-Mn**) shows different redox behaviors than **NP2-Si** and **NP2-Cu**, because **NP2-Mn** has redox active metal center (Mn³⁺). For this reason, **NP2-Mn** shows metal-based reduction processes in addition to the phthalocyanine ring-based electron transfer reactions [35–37]. Here **NP2-Mn** shows two metal-based reductions at −0.17 V (R1), −1.01 V (R2) and one phthalocyanine ring-based reduction at −1.51 V (R₃) during the cathodic potential scans. On the other hand, during the anodic potential scans, one phthalocyanine ring-based oxidation at 1.19 V (O₁) is observed. According to the peak-to-peak separation (ΔE_P), R₁ has reversible, R₂, R₃ and O₁ have quasi-reversible character.

4. Conclusion

In this work, Si(IV), Cu(II), Mn(III) phthalocyanines substituted with (4-[(1E)-(4 methoxyphenyl) methylene] aminophenoxy) groups were synthesized and analyzed by FT-IR, NMR, UV-Vis, mass spectroscopy. The redox behaviors of axially di- and peripherally tetra-(4-{[(1E)-(4-methoxyphenyl)methylene]amino}phenoxy) group substituted metallophthalocyanines were determined. Electrochemical results of **NP2-Si, NP2-Cu, NP2-Mn** were in compatible with the responses of the similar metallophthalocyanines. While **NP2-Si** and **NP2-Cu**, only showed phthalocyanine ring based redox processes, **NP2-Mn** showed rich redox responses and both metal-based and phthalocyanine ring based redox processes. **NP2-Mn** showed two metal-based and one phthalocyanine ring-based reduction reactions. The addition of Mn³⁺ cation to the phthalocyanine ring significantly changed the redox richness of phthalocyanines.

Acknowledgement

References

[1] N. Kayir, S. Gorduk, Synthesis, characterization, and investigation photophysicochemical properties of axially 2-hydroxymethyl-1,4-benzodioxan di-substituted Silicon(IV) phthalocyanine, J Organomet Chem, 990, 2023, 122661.

[2] R. Balamurugan, J.H. Liu, B.T. Liu, A review of recent developments in fluorescent sensors for the selective detection of palladium ions, Coord Chem Rev, 376, 2018, 196–224.

[3] T. Arslan, N. Çakır, T. Keleş, Z. Biyiklioglu, M. Senturk, Triazole substituted metal-free, metallo-phthalocyanines and their water soluble derivatives as potential cholinesterases inhibitors: Design, synthesis and in vitro inhibition study, Bioorg Chem, 90, 2019, 103100.

[4] S. Temizel, T.Ç. Çanak, A.M. Sevim, Novel polymers with cobalt(II)phthalocyanine moieties as effective heterogeneous photocatalysts for visible-light-driven photodegradation of organic dyes in aqueous solutions, J Photochem Photobiol A Chem, 401, 2020, 112741.

[5] R. Ishiura, A. Fujii, M. Arita, K. Sudoh, M. Ozaki, Study on energy level bending at heterojunction of solution-processed phthalocyanine thin film and n-Si by Kelvin probe force microscopy, Org Electron, 78, 2020, 105599.

[6] R. Zugle, T. Nyokong, Physico-chemical properties of lutetium phthalocyanine complexes in solution and in solid polystyrene polymer fibers and their application in photoconversion of 4-nitrophenol, J Mol Catal A Chem, 358, 2012, 49–57.

[7] M. Yahya, Y. Nural, Z. Seferoğlu, Recent advances in the nonlinear optical (NLO) properties of phthalocyanines: A review, Dye Pigment, 198, 2022, 109960.

[8] E. Güzel, H. Baş, Z. Biyiklioglu, İ. Şişman, Dye-sensitized solar cells using silicon phthalocyanine photosensitizers with pyridine anchor: Preparation, evaluation of photophysical, electrochemical, and photovoltaic properties, Appl Organomet Chem, 35, 2021,.

[9] B. Yıldız, B.S. Arslan, E. Güzel, M. Nebioğlu, N. Menges, İ. Şişman, M. Kasım Şener, Non-aggregating zinc phthalocyanine sensitizer with bulky diphenylphenoxy donor groups and pyrazole-3-carboxylic acid anchoring group for coadsorbent-free dye-sensitized solar cells, Sol Energy, 226, 2021, 173–179.

[10] Z. Biyiklioglu, H. Bas, H. Alp, Non-aggregated axially disubstituted silicon phthalocyanines bearing electropolymerizable ligands and their aggregation, electropolymerizaton and thermal properties, Dalt Trans, 44, 2015, 14054–14062.

[11] Z. Biyiklioglu, H. Alp, Electropolymerizable peripherally tetra-{2-[3-(diethylamino)phenoxy]ethoxy} substituted as well as axially (4-phenylpiperazin-1-yl)propanoxy-disubstituted silicon phthalocyanines and their electrochemistry, Dalt Trans, 44, 2015, 18993–18999.

[12] Z. Biyiklioglu, I. Ömeroğlu, H. Alp, Synthesis, characterization and electrochemical properties of amphiphilic axially-disubstituted silicon(IV) phthalocyanines, J Coord Chem, 69, 2016, 354–362.

[13] Y. Baygu, Y. Gök, Synthesis and characterization of new partially-aggregated water-soluble polyether-triazole linked zinc(II) phthalocyanines as photosensitizers for PDT studies, Synth Met, 260, 2020, 116256.

[14] H. Kantekin, H. Yalazan, B. Barut, Ö. Güngör, D. Ünlüer, Ü. Demirbaş, A. Özel, M. Durmuş, Dual-purpose both peripheral and non-peripheral triazole substituted ZnII, MgII and PbII phthalocyanines: Synthesis, characterization, photophysicochemical and acetylcholinesterase inhibitory properties, Polyhedron, 208, 2021, 115416.

[15] A. Günsel, A.T. Bilgiçli, B. Barut, P. Taslimi, A. Özel, İ. Gülçin, Z. Biyiklioglu, M.N. Yarasir, Synthesis of water soluble tetra-substituted phthalocyanines: Investigation of DNA cleavage, cytotoxic effects and metabolic enzymes inhibition, J Mol Struct, 1214, 2020, 128210.

[16] Z. Bıyıklıoğlu, V. Çakır, D. Çakır, H. Kantekin, Crown ether-substituted water soluble phthalocyanines and their aggregation, electrochemical studies, J Organomet Chem, 749, 2014, 18–25.

[17] R. Atajanov, B. Huraibat, Z. Odabaş, A.R. Özkaya, Electrochemical, spectroelectrochemical, and electrocatalytic properties of novel soluble phthalocyanines containing peripheral thymoxy and chloride units, Inorganica Chim Acta, 547, 2023, 121360.

[18] H. Baş, Z. Biyiklioglu, B. Barut, C.Ö. Yalçın, A. Özel, Highly water soluble axial disubstituted silicon(IV) phthalocyanine, naphthalocyanine: Synthesis, DNA interaction and anticancer effects against human lung (A549), liver (SNU-398), melanoma (SK-MEL128), prostate (DU-145), breast (BT-20) cell lines, Inorg Chem Commun, 156, 2023, 111139.

[19] A. Günsel, P. Taslimi, G.Y. Atmaca, A.T. Bilgiçli, H. Pişkin, Y. Ceylan, A. Erdoğmuş, M.N. Yarasir, İ. Gülçin, Novel potential metabolic enzymes inhibitor, photosensitizer and antibacterial agents based on water-soluble phthalocyanine bearing imidazole derivative, J Mol Struct, 1237, 2021, 130402.

[20] S.M. Sudhakara, M.C. Devendrachari, F. Khan, S. Thippeshappa, H.M.N. Kotresh, Highly sensitive and selective detection of nitrite by polyaniline linked tetra amino cobalt (II) phthalocyanine surface functionalized ZnO hybrid electrocatalyst, Surfaces and Interfaces, 36, 2023, 102565.

[21] R.A. Shoukat Ali, J. Keshavayya, A.S. Jagadisha, S.D. Umesha, K.N. Gujjar, S.A. Narasimha, D.G. Prasanna, E. Nagaraja, DC electrical conductivity studies of tetra 2-(furan-2-yl)-1,3,4-oxadiazole substituted metal (II) phthalocyanines, Mater Today Proc, 49, 2022, 644–649.

[22] M.-R. Ke, J.-D. Huang, S.-M. Weng, Comparison between non-peripherally and peripherally tetra-substituted zinc (II) phthalocyanines as photosensitizers: Synthesis, spectroscopic, photochemical and photobiological properties, J Photochem Photobiol A Chem, 201, 2009, 23–31.

[23] D. AlMarzouq, S. A. Majeed, Ö. Budak, A. Koca, Manganese phthalocyanine and its graphene quantum dot conjugate: Synthesis, characterization electrochemistry, spectroelectrochemistry, electropolymerization, and electrochromism, Inorganica Chim Acta, 527, 2021, 120558.

[24] Y. Ünver, H. Baş, Z. Biyiklioglu, Non-peripherally 4-{[(1E)-1-benzothien-2-ylmethylene]amino}phenol substituted zinc(II), manganese(III), cobalt(II) phthalocyanines: Synthesis and electrochemistry, J Mol Struct, 1178, 2019, 508–513.

[25] S. Gorduk, A. Altindal, Non-peripherally tetra substituted phthalocyanines bearing carboxylic acid anchoring groups as photosensitizer for high efficient dye-sensitized solar cells, J Mol Struct, 1204, 2020, 127636.

[26] S. Gorduk, Investigation of photophysicochemical properties of non-peripherally tetra-substituted metal-free, Mg(II), Zn(II) and In(III)CI phthalocyanines, Polyhedron, 189, 2020, 114727.

[27] R. Bayrak, H.T. Akçay, Z. Bıyıklıoğlu, İ. Değirmencioğlu, Substituted phthalocyanines and their electropolymerization properties, Synth Met, 220, 2016, 643–652.

[28] M. Shumba, T. Nyokong, Electrode modification using nanocomposites of boron or nitrogen doped graphene oxide and cobalt (II) tetra aminophenoxy phthalocyanine nanoparticles, Electrochim Acta, 196, 2016, 457–469.

[29] Ö. Kurt, A. Koca, A. Gül, M. Burkut Koçak, Synthesis, electrochemistry and in situ spectroelectrochemistry of novel hexadeca-substituted phthalocyanines with three different groups, Synth Met, 206, 2015, 72–83.

[30] A. Günsel, M. Kandaz, A. Koca, B. Salih, Peripheral and non-peripheral-designed multifunctional phthalocyanines; synthesis, electrochemistry, spectroelectrochemistry and metal ion binding studies, Polyhedron, 30, 2011, 1446–1455.

[31] G.H. Hegazy, H.I. Ali, Design, synthesis, biological evaluation, and comparative Cox1 and Cox2 docking of p-substituted benzylidenamino phenyl esters of ibuprofenic and mefenamic acids, Bioorg Med Chem, 20, 2012, 1259–1270.

[32] H. Fazlı, Ç. Akkol, S.C. Osmanoğulları, Z. Biyiklioglu, E.T. Saka, O. Bekircan, Synthesis of water soluble copper(II), manganese(III) phthalocyanines and their photocatalytic performances in benzyl alcohol photoxidation, J Organomet Chem, 983, 2023, 122553.

[33] Z. BIYIKLIOĞLU, H. BAŞ, Synthesis and effect of substituent position, metal type on the electrochemical properties of (3-morpholin-4-ylpropoxy) groups substituted cobalt, manganese phthalocyanines, TURKISH J Chem, 44, 2020, 687–694.

[34] G. Gümrükçü Köse, G.K. Karaoğlan, Y. Erdağ Maden, A. Koca, Novel silicon phthalocyanine photosensitizers containing carboxylic acid based axial anchoring groups: Electrochemistry, spectroelectrochemistry, and dye sensitized solar cell performance, Dye Pigment, 207, 2022, 110686.

[35] H. Yalazan, Y.E. Maden, A. Koca, H. Kantekin, Multi-step syntheses, electrochemistry and spectroelectrochemistry of peripheral CoII, CuII and MnIIICl phthalocyanines bearing pyrazoline, J Mol Struct, 1269, 2022, 133788.

[36] D. Akyüz, Ü. Demirbaş, O. Bekircan, Metallo-phthalocyanines Containing 1,3,4-oxadiazole Substituents: Synthesis, Characterization, Electrochemical and Spectroelectrochemical Properties, ChemistrySelect, 8, 2023, e20220459.

[37] G. Dilber, A. Nas, Ö. Budak, A. Koca, Chloromanganese and oxo-Titanium (IV) phthalocyanines: Synthesis, electrochemistry and Spectroelectrochemistry, Polyhedron, 242, 2023, 116495.